

**Estimation of Burst Pressure of Corroded Pipeline Using Finite Element Analysis  
(FEA)**

by

**Mohamad Armiya bin Zahari**

Dissertation submitted in partial fulfillment of

the requirement for the

**Bachelor of Engineering (Hons)**

**(Mechanical Engineering)**

**SEPTEMBER 2011**

**Universiti Teknologi PETRONAS  
Bandar Seri Iskandar  
31750 Tronoh  
Perak Darul Ridzuan**

**CERTIFICATION OF APPROVAL**

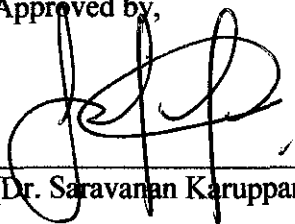
**Estimation of Burst Pressure of Corroded Pipeline Using Finite Element Analysis  
(FEA)**

by

**Mohamad Armiya bin Zahari**

A project dissertation submitted to the  
Mechanical Engineering Programme  
Universiti Teknologi PETRONAS  
in partial fulfillment of the requirement for the  
**BACHELOR OF ENGINEERING (Hons)**  
**(MECHANICAL ENGINEERING)**

Approved by,



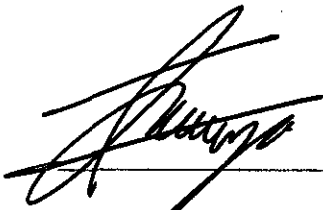
(Dr. Saravanan Karuppanan)

**UNIVERSITI TEKNOLOGI PETRONAS  
TRONOH, PERAK**

**SEPTEMBER 2011**

## CERTIFICATION OF ORIGINALITY

This is to certify that I am responsible for the work submitted in this project, that the original work is my own except as specified in the references and acknowledgements, and that the original work contained herein have not been undertaken or done by unspecified sources or persons.



---

MOHAMAD ARMIYA BIN ZAHARI

## ABSTRACT

Pipelines are used to transmit fluid from one point to another. One major concern of maintaining pipelines integrity is failure due to corrosion defects. Corrosion is one of the common defects in pipes which can be observed externally or internally. Several methods and codes had been established to provide solutions in assessing the corroded pipes. This includes the assessment of remaining strength of the corroded pipeline which has been used for used in decades, ASME B31G. This code is referred in evaluation of metal loss in pressurized pipes and piping systems. Another code, the recommended practice DNV-RP-F101 is used to evaluate the remaining strength of corroded pipes which has single defect, multiple defects and complex shape defects.

This study is associated with the process to estimate the burst pressure of corroded pipeline by using Finite Element Analysis (FEA). The corroded pipe undergoes UT-Scan and the thickness along the pipe's internal surface is measured and the corrosion profile is plotted. FEA is used to resemble the experimental procedure of actual burst test. Several models are built and simulated by considering defect shape, defect depth and analysis type as parameter to distinguish every simulations. All models are properly constraint and pressurized internally thus, the maximum allowable burst pressure ( $P_b$ ) of corroded pipeline is determined. The result obtained by FEA is analyzed, studied and compared with the actual burst test, ASME B31G and DNV-RP-F101. Lastly, the best model of ANSYS simulation is determined from the simulation.

## **ACKNOWLEDGEMENTS**

I would like to forward my utmost gratitude to my supervisor, Dr. Saravanan Karuppanan for his weekly advices and guidance throughout the whole Final Year Project (FYP) period. With that, this project was going smoothly as planned and successfully finished.

My heartiest appreciation goes to my examiners for their constructive comments and criticisms, and also not to be left behind, my parents and all my friends who had given me endless support towards completing the Final Year Project.

Thank you.

## NOMENCLATURE

FEA	Finite Element Analysis
FEM	Finite Element Method
RSTRENG	Remaining Strength of Corroded Pipe
API	American Petroleum Institute
UT	Ultrasonic Testing
ASME	American Society of Mechanical Engineer
DNV-RP	Det Norske Veritas- Recommended Practice
SMYS	Specified Minimum Yield Strength
$\sigma_{VonMises}$	Von Mises Stress
$\sigma_{SMYS}$	Specified Minimum Tensile Strength
$\sigma_{axial}$	Axial Tension
$P$	Internal Pressure loading
$P_b$	Burst pressure
$r$	Radius
$t$	Thickness

## TABLE OF CONTENTS

<b>CERTIFICATION OF APPROVAL</b>	.	.	.	.	.	.	.	<b>i</b>
<b>CERTIFICATION OF ORIGINALITY</b>	.	.	.	.	.	.	.	<b>ii</b>
<b>ABSTRACT</b>	.	.	.	.	.	.	.	<b>iii</b>
<b>ACKNOWLEDGEMENTS</b>	.	.	.	.	.	.	.	<b>iv</b>
<b>NOMENCLATURE</b>	.	.	.	.	.	.	.	<b>v</b>
<b>TABLE OF CONTENTS</b>	.	.	.	.	.	.	.	<b>vi</b>
<b>LIST OF FIGURES</b>	.	.	.	.	.	.	.	<b>ix</b>
<b>LIST OF TABLES</b>	.	.	.	.	.	.	.	<b>xi</b>
<b>CHAPTER 1: INTRODUCTION</b>	.	.	.	.	.	.	.	<b>1</b>
1.1 Background of study	.	.	.	.	.	.	.	<b>1</b>
1.2 Problem statement.	.	.	.	.	.	.	.	<b>2</b>
1.3 Objectives .	.	.	.	.	.	.	.	<b>3</b>
1.4 Scope of study	.	.	.	.	.	.	.	<b>3</b>
<b>CHAPTER 2: LITERATURE REVIEW</b>	.	.	.	.	.	.	.	<b>4</b>
<b>CHAPTER 3: METHODOLOGY</b>	.	.	.	.	.	.	.	<b>9</b>
3.1 Experimental data .	.	.	.	.	.	.	.	<b>10</b>
3.2 Codes and Equations	.	.	.	.	.	.	.	<b>11</b>
3.2.1 ASME B31G	.	.	.	.	.	.	.	<b>12</b>
3.2.2 DNV-RP-F101	.	.	.	.	.	.	.	<b>13</b>

3.3 ANSYS Software . . . . .	15
3.3.1 Familiarization of ANSYS . . . . .	16
3.3.2 Modeling . . . . .	16
3.3.2.1 Model 1 . . . . .	17
3.3.2.2 Model 2 . . . . .	18
3.3.2.3 Model 3 . . . . .	19
3.3.2.4 Model 4 . . . . .	19
3.3.2.5 Model 5 . . . . .	20
3.3.2.6 Model 6 . . . . .	20
3.3.2.7 Model 7 . . . . .	20
3.3.2.8 Model 8 . . . . .	21
3.3.2.9 Model 9 . . . . .	21
3.3.3 Meshing . . . . .	22
3.3.4 Symmetric boundary conditions and Loads	
Application . . . . .	23
3.4 Project schedule . . . . .	26
<b>CHAPTER 4: RESULTS AND DISCUSSIONS . . . . .</b>	<b>27</b>
4.1 ANSYS post processing results . . . . .	27
4.2 Discussions . . . . .	36
<b>CHAPTER 5: CONCLUSION AND RECOMMENDATIONS . . . . .</b>	<b>39</b>



5.1 Conclusion	. . . . .	39
5.2 Recommendations.	. . . . .	39
<b>REFERENCES</b>	. . . . .	<b>40</b>
<b>APPENDICES</b>	. . . . .	<b>42</b>
Appendix I: FYP I Project Gantt Chart	. . . . .	42
Appendix II: FYP II Project Gantt Chart	. . . . .	43
Appendix III: Tensile Properties of API X52 grade steel [6]	. . . . .	45
Appendix IV: Mesh of Model 1, 3 and 4	. . . . .	46
Appendix V: Mesh of Model 2, 5 and 6	. . . . .	46
Appendix VI: Mesh of Model 7 and 8	. . . . .	47
Appendix VII: Mesh of Model 9	. . . . .	47

## LIST OF FIGURES

Figure 2.1: Burst pressure versus the empirical function of geometric parameters and the best linear fit [2] . . . . .	5
Figure 2.2: Comparison between experiments, the linear fit, and predictions from DNV and B31G codes [2] . . . . .	6
Figure 2.3: Internal and external defects [3]. . . . .	6
Figure 2.4: Stress Distribution [3] . . . . .	7
Figure 2.5: Deformation stages of burst [3] . . . . .	7
Figure 3.1: Flow diagram of project . . . . .	9
Figure 3.2: Pipe's Dimension . . . . .	10
Figure 3.3: Corrosion region profile. . . . .	11
Figure 3.4: Model 1 . . . . .	17
Figure 3.5: Idealized geometry of Model 1 . . . . .	17
Figure 3.6: Model 2 . . . . .	18
Figure 3.7: Idealized geometry of Model 2 . . . . .	19
Figure 3.8: Model 7 . . . . .	20
Figure 3.9: Idealized geometry of Model 7 . . . . .	21
Figure 3.10: Model 9 . . . . .	22
Figure 3.11: Idealized geometry of Model 9 . . . . .	22
Figure 3.12: Symmetric boundary conditions application . . . . .	24
Figure 3.13: Internal pressure loading . . . . .	25

Figure 3.14: Axial load (red arrow)	26
Figure 4.1: Von Misses plot for Model 1	27
Figure 4.2: Von Misses plot for Model 2	28
Figure 4.3: Von Misses plot for Model 3	29
Figure 4.4: Von Misses plot for Model 4	30
Figure 4.5: Von Misses plot for Model 5	31
Figure 4.6: Von Misses plot for Model 6	32
Figure 4.7: Von Misses plot for Model 7	33
Figure 4.8: Von Misses plot for Model 8	34
Figure 4.9: Von Misses plot for Model 9	35
Figure 4.10: Comparisons of FEA to Actual burst test, ASME B31G and DNV-RP-F101	38

## LIST OF TABLES

Table 2.1: Comparison of failure pressure obtained by tests and finite element analysis [4]	8
Table 3.1: Pipe's specification and mechanical properties	10
Table 3.2: Model 1 dimensions and material properties	18
Table 3.3: Model 2 dimensions and material properties	19
Table 3.4: Model 7 dimensions	21
Table 3.5: Meshing properties	23
Table 4.1: Simulation results for Model 1	28
Table 4.2: Simulation results for Model 2	29
Table 4.3: Simulation results for Model 3	30
Table 4.4: Simulation results for Model 4	31
Table 4.5: Simulation results for Model 5	32
Table 4.6: Simulation results for Model 6	33
Table 4.7: Simulation results for Model 7	34
Table 4.8: Simulation results for Model 8	35
Table 4.9: Simulation results for Model 9	36
Table 4.10: Comparisons of burst pressure, $P_b$	37

# CHAPTER 1

## INTRODUCTION

### 1.1 Project background

#### 1.1.1 Pipeline

Pipeline is a way to transmit fluid from one point to another through pipes. Pipeline had been used for oil and gas transmission all over the world nowadays. It is the reliable and safest way to transmit the product to be processed in the plant and distributed later to the customers. The major concern of the pipeline is maintaining its integrity to ensure it is safe and effective while operating to avoid unforeseen failure. One of the pipeline integrity issues to be concerned is corrosion defects. This is a main problem because material used in pipeline is carbon steel which is being classified as alloy and it will be exposed to the corrosion attack either fast or slow depending on the environment conditions.

#### 1.1.2 Corrosion

Corrosion is the deterioration of a material or metal because of its reaction with environment. It happens when there are anode, cathode, metallic path and electrolyte at the metal [1]. Further studies had been done to avoid the corrosion to attack metal or to delay the process and it is applied in oil and gas industry, manufacturing, civil engineering and many more. Pipeline which is made of carbon steel also faces the problem on corrosion attack. Corrosion will deteriorate the pipes and causes the metal loss on the pipe's surface. After a certain period, the metal loss on the surface will be greater and at the end, the pipes will crack and leak. If the incident happens, for example in a pipeline

with fluid flowing with high pressure, the pipe may burst and may cause operation shutdown, equipment failure and injury to the surrounding people. Hence, the burst pressure of the corroded pipeline has to be estimated so that precaution can be taken to avoid any accidents to happen.

### **1.1.3 Burst pressure**

Burst pressure is the maximum pressure that the pipes can sustain before they burst or it may also be defined as the point right before failure occurs. Some factors that contribute to determination of the burst pressure are the material quality, thickness of the pipes, heat and many more. To determine the burst pressure of a pipe, a test must be done where the pipe is pressurized until it burst and the burst pressure is recorded which is done in a lab. Beside the experimental method, the burst pressure can also be found or estimated by using Finite Element Analysis (FEA) which will be discussed further.

## **1.2 Problem Statement**

As a pipeline ages, it can be affected by corrosion mechanisms, which may lead to decrease in its structural integrity and eventual failure. One of the main reasons of the eventual failure is corrosion defects. Pipeline will deteriorate or corrode either fast or slowly. This is due to insufficient external coating protection and environmental influence which affect the cathodic protection. The loss of metal on a pipeline due to corrosion, usually results in localized pits with different depths and uneven shapes on its external and internal surfaces [1]. Consequently, intensive research and study have been carried out to assess the pipeline structural integrity to give precise suggestion to estimate the failure pressure or burst pressure of pipeline.

One of the tests carried out for the purpose of this assessment is burst test. A sample of corroded pipe will be pressurized until it burst and the data of the

maximum allowable burst pressure will be analyzed and the integrity of pipeline can be determined. But, the problem for the test is it can't be done for all pipes along the pipeline due to time constraint, cost and safety reasons. In order to overcome this matter, the author is going to estimate the burst pressure using Finite Element Analysis (FEA) and uses ANSYS software for that purposes.

### **1.3 Objectives**

The objectives of this project are:

- a) To estimate the maximum allowable burst pressure ( $P_b$ ) of corroded pipeline by Finite Element Analysis (FEA).
- b) To compare the result obtained by FEA with the experimental values and determine the best model for ANSYS simulation of corroded pipeline.

### **1.4 Scope of study**

The FEA is started by assembling the results of UT-Scan, followed by the plotting of the corrosion profile where the corrosion pits area and the deepest pits are known. With this profile, the corroded pipe segment will be generated in several 3-D models with different shapes, depth and analysis type. The modelling process use ANSYS software and the models will be meshed, constrained and internally pressurized until the burst pressure is determined. The result of the FEA will be compared to the experimental values and the best model to be used for this project is then determined.

## CHAPTER 2

### LITERATURE REVIEW

Extensive studies have been conducted to assess the integrity of pipes containing wall thinning because of corrosion defects under internal pressure. This includes the burst tests which were carried out experimentally in the lab. For this test, researchers had to face some obstacles including the cost of the test, safety precaution and the lengthy procedures to gather the results. Apparently, computer technology which had evolved in human activity had given the alternative way for the assessment to be accomplished in order to minimize the cost of the burst test and to save time to analyze the data. By conducting the Finite Element Analysis (FEA) using structural analysis software researchers are able to estimate the burst pressure of corroded pipelines.

A research had been carried out by T.A. Netto, U.S. Ferraz and S.F. Estefen [2] on the effects of corrosion defects on the burst pressure of pipeline. In their research, they had performed the work in physical experiment as well as the numerical analysis using FEA software ABAQUS. Several pipes with corrosion defects are tested for the burst pressure and every pipe was idealized with the corrosion defects shapes on it and simulated in the computer. ASME B31G and DNV- RP- F101 are used as their references codes of their research.

They had used 3 types of pipes with grade API X52, API X65 and API X77. They found that the burst pressure is dependent on the major parameters and after conducting parametric study on the pipes, they simplified into an equation:

$$\frac{P_b}{P_{bi}} = 1 - 0.9435 \left( \frac{d}{t} \right)^{1.6} \left( \frac{l}{D} \right)^{0.4}$$



where,

$P_b$  = burst pressure of the corroded pipe

$P_{bi}$  = burst pressure of intact pipe

$D$  = outside diameter of the pipe

$t$  = wall thickness of the pipe

$d$  = maximum depth of the defect

$l$  = maximum length of the defect

The numerical results are plotted using the equation above as shown in **Figure 2.1**.

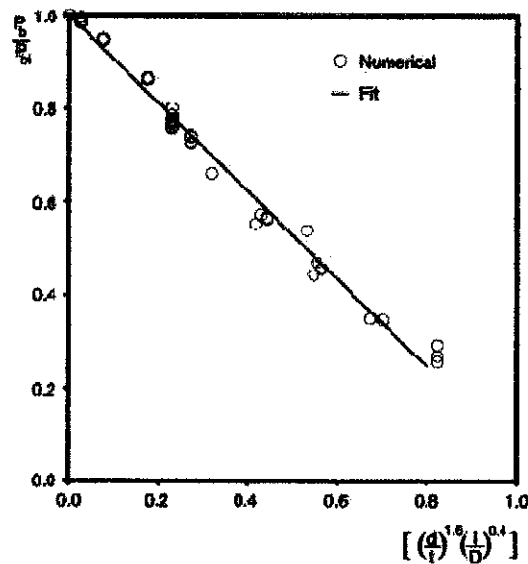


**Figure 2.1:** Burst pressure versus the empirical function of geometric parameters and the best linear fit [2]

After that, the ASME B31G, DNV-RP-F101 and the FEA results are compared as shown in **Figure 2.2**.

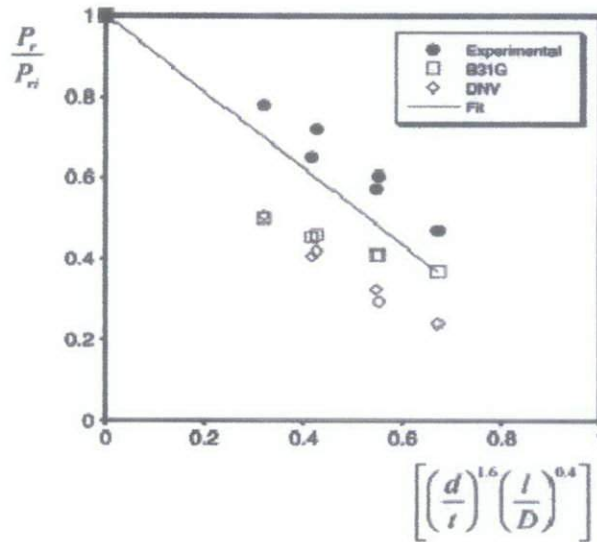


**Figure 2.2:** Comparison between experiments, the linear fit, and predictions from DNV and B31G codes [2]

Tomas Szary [3] in his thesis highlighted the development of the numerical model using ANSYS. **Figure 2.3** shows the model generation of defects with quarter of the exact pipe dimension. Meshing of the model is described later by using 10 mm size of elements. Then, the author described the applied loads which are namely internal, external pressure and axial load. Ovality of the pipe also was taken into consideration. Special emphasis was put on realistic defect modeling where the descriptions of limitations, boundary conditions and FEM model characteristics are discussed. The author put also different samples of model with different defects shapes in his project.

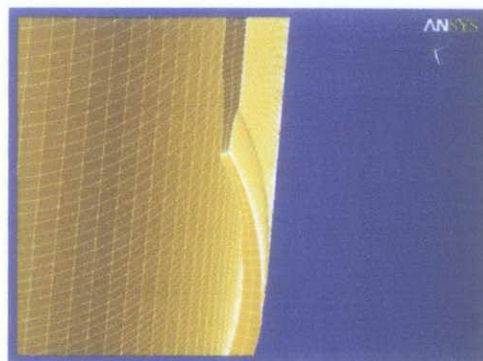


**Figure 2.3:** Internal and external defects [3]

The author also presented respectively the burst analysis he had done. The author had simplified the steps of the analysis with a developed procedure where all the parameter and variable input is in a specific window. The deformation stages and the stress distribution are illustrated in **Figure 2.4 and 2.5**. Consequently, model validations and comparison to tests and other existing corrosion method assessments are presented. They are dependent on defect geometry and material properties. The defect shape plays an important role because it influences stress distribution. Finally, the author made a comparison in his analysis of the FEA result with other codes which are manually calculated using the formula given. The codes include API 5CT, ASME B31.8, RSTRENG 0.85dl.

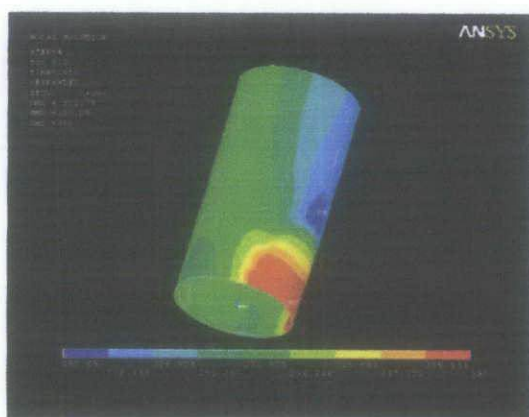


**Figure 2.4:** Stress Distribution [3]

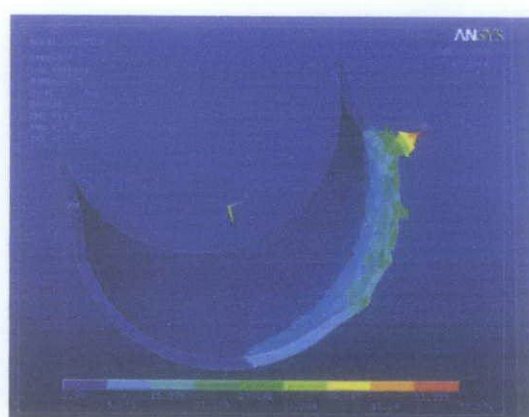


**Figure 2.5:** Deformation stages of burst [3]

Another research was conducted by M. Kamayaa, T. Suzuki, and T. Meshii [4] on the estimation of the burst pressure, where they discussed the importance of plastic deformation consideration to estimate the burst pressure before bursting occurs. 3D elastic–plastic FEA was conducted to examine the influence of the material and length of wall thinning on the failure pressure. Wall thinning was assumed to be of uniform depth circumferentially inside the straight pipe. Besides, they try to evaluate the influence of the material and flaw length on the experimental results. FEA to estimate the burst pressure was initially conducted by assuming the different flaw lengths and

materials of pipe, but with same pipe dimensions and constant flaw depth. The validity of FEA was confirmed by comparing its results with the experimental results obtained from previous study as stated in **Table 2.1**.

**Table 2.1:** Comparison of failure pressure obtained by tests and finite element analysis  
[4]

<b>Length of flaw (mm)</b>	<b>Burst Test (MPa)</b>	<b>FEA (MPa)</b>
72.5	17.49	17.90
50	18.07	18.13
25	23.90	22.90

## CHAPTER 3

### METHODOLOGY

Several steps were taken to develop the FEA simulations to accomplish this project. The overall methodology is illustrated in a flow diagram form shown in **Figure 3.1** below.

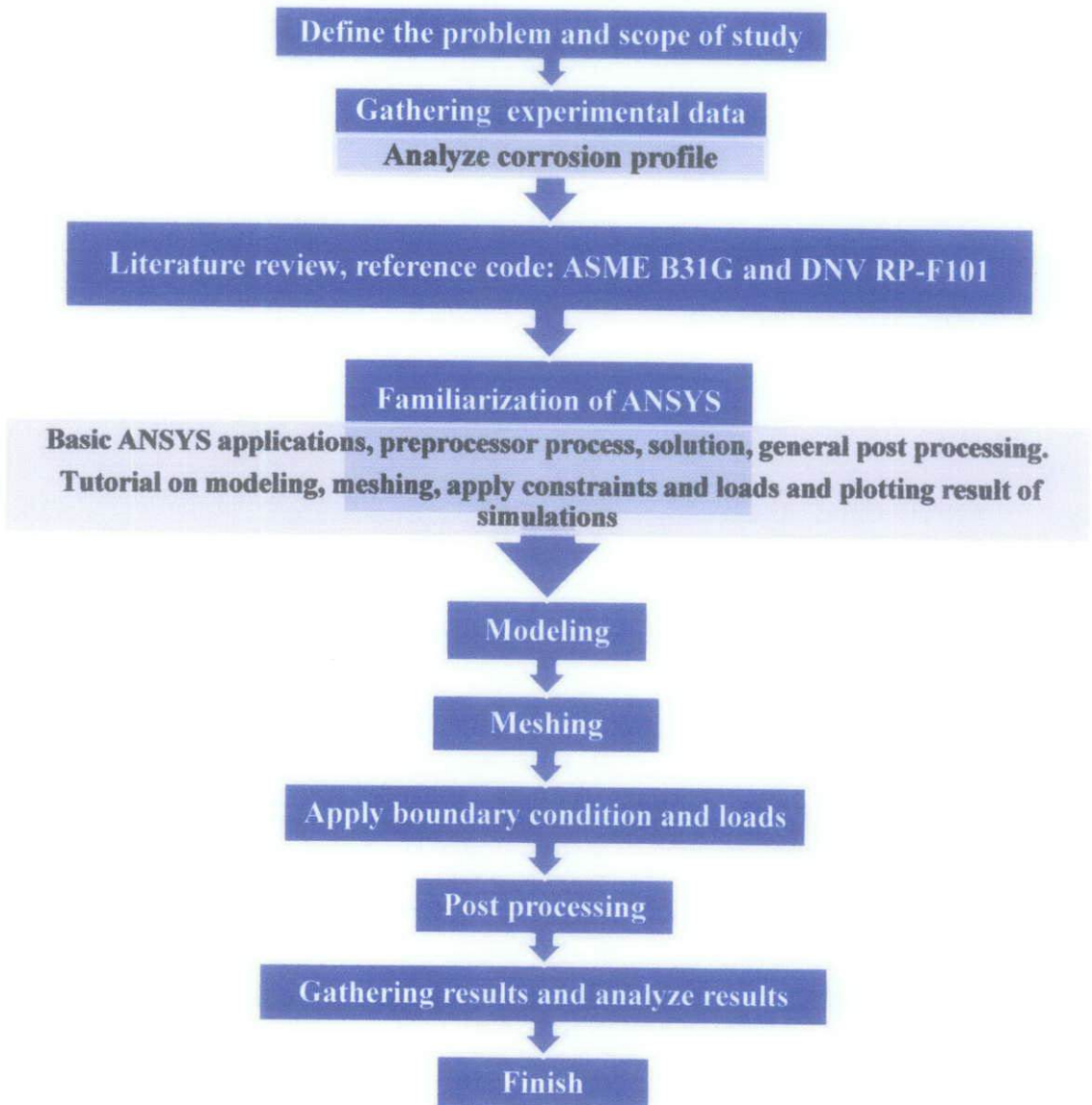


**Figure 3.1:** Flow diagram of project

### 3.1 Experimental data

The burst test was conducted experimentally in the Universiti Teknologi PETRONAS's lab. The pipe segment is illustrated in **Figure 3.2** and the pipe's specification and material properties is presented in **Table 3.1**.

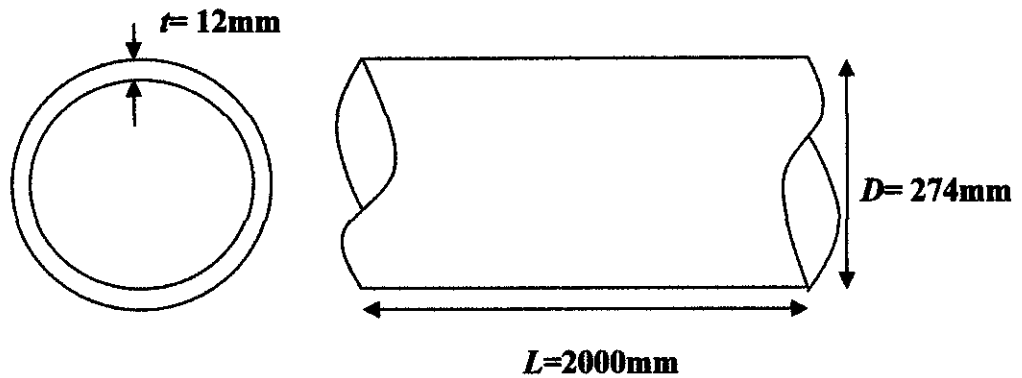


**Figure 3.2:** Pipe's Dimension

**Table 3.1:** Pipe's specification and mechanical properties

Nominal Outside Diameter, $D$	274 mm
Wall thickness, $t$	12 mm
Length, $L$	2000 mm
Material Grade	API 5L X52
Specified Minimum Yield Strength, SMYS	358 MPa
Specified Minimum Tensile Strength, SMTS	455 MPa

The corrosion region profile is plotted as in **Figure 3.3** after UT Scan result is obtained. From the pipe profile, the minimum wall thickness is 7.58mm and the



deepest defect depth is 4.42mm. The low thickness area will be idealized into geometries of corrosion pits area (red square) for all models.

### Pipe's thickness profile

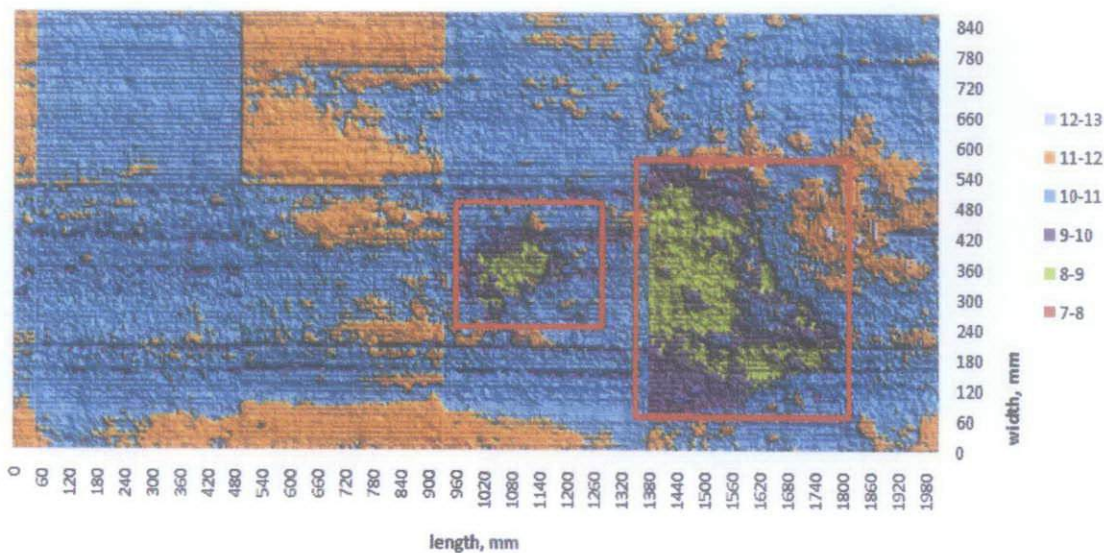


**Figure 3.3:** Corrosion region profile

Based on this profile, the model of corroded pipe is built. The modeling is based on the corrosion profile above by taking the defect depth, defect geometry and analysis type as parameter in this study.

## 3.2 Codes and Equations

In this project, two codes are used to evaluate the strength of corroded pipe in engineering and industrial practices which are ASME B31G and DNV-RP-F101. Those codes are studied and understood as a guideline to estimate the Maximum Allowable Burst Pressure of corroded pipeline by using FEA.

### 3.2.1 ASME B31G

ASME B31G is the manual for determining the remaining strength of corroded pipeline [5]. This code is referred for the purpose of providing guidance in the evaluation of metal loss in pressurized pipelines and piping systems. The equations in this manual were developed based upon pressuring actual corroded pipe to failure in an extensive series of full-size tests. It is applicable to all pipelines and piping systems that are part of ASME B31 Code for Pressure Piping. With this code, safe maximum pressure for corroded pipelines can be determined.

The steps for determining Maximum Allowable Operating Pressure are:

- i) Computation of Projected Area of Corrosion,  $A$

$$A = 0.893 \left( \frac{L_m}{\sqrt{Dt}} \right) \quad (\text{Eq. 1})$$

- ii) Computation of  $P$

$$P = 2StFT / D \quad (\text{Eq. 2})$$

- iii) Computation of Safe Maximum Pressure,  $P'$

$$P' = 1.1P \left[ \frac{1 - \frac{2}{3} \left( \frac{d}{t} \right)}{1 - \frac{2}{3 \left( \frac{d}{t\sqrt{A^2+1}} \right)}} \right] \quad (\text{Eq. 3})$$



where,

$A$  = Projected area of corrosion in the longitudinal plane through the wall thickness (mm<sup>2</sup>)

$d$  = Depth of corroded region (mm)

$L_m$  = Longitudinal length of corroded region (mm)

$t$  = Uncorroded, pipe wall thickness (mm)

$D$  = Nominal outside diameter (mm)

$P'$  = The safe maximum pressure of corroded area

$P$  = The greater of either the established MAOP (Maximum Allowable Operating Pressure)

$S$  = Specified minimum yield strength (SMYS)

$F$  = Appropriate design factor

$T$  = Temperature derating factor

### 3.2.2 DNV-RP-F101

DNV stands for Det Norske Veritas and RP (Recommended Practice) gives recommendations to assess corroded pipelines subject to internal pressure, and internal pressure combined with longitudinal compressive stresses which cover single defects, interacting defects and complex

shaped defects [6]. DNV-RP-F101 proposes two methods to find the failure pressure. The first method is named the calibrated safety factor method, and the second is classified as the allowable stress design (ASD) format.

For this project, the equations of longitudinal corrosion defect subjected to internal pressure loading are used. Therefore the Maximum Allowable Corroded Pressure can be determined from the equations below:

- i) Calculation of Maximum Acceptable Defect Depth  $(d/t)^*$

$$(d/t)^* = (d/t)_{\text{means}} + \epsilon_a StD [d/t]$$

(Eq. 4)

- ii) Calculation of Length Correction Factor,  $Q$

$$Q = \sqrt{1 + 0.31 \left( \frac{L}{\sqrt{DT}} \right)^2}$$

(Eq. 5)

- iii) Calculation of Maximum Allowable Corroded Pressure,  $P_{\text{corr}}$

$$P_{\text{corr}} = \frac{\gamma_m 2 t f_u (1 - \gamma_d (d/t)^*)}{(D - t) \left( 1 - \frac{\gamma_d (d/t)^*}{Q} \right)}$$

(Eq. 6)

where,

- $A_c$  = Projected area of corrosion in the circumferential plane through the wall thickness ( $\text{mm}^2$ )
- $P_{corr}$  = Allowable corroded pipe pressure of a single longitudinal corrosion defect under internal pressure loading ( $\text{N}/\text{mm}^2$ )
- $d$  = Depth of corroded region (mm)
- $L$  = Longitudinal length of corroded region (mm)
- $t$  = Pipe wall thickness (mm)
- $D$  = Nominal outside diameter (mm)
- $\gamma_m$  = Partial safety factor for longitudinal corrosion prediction
- $\gamma_d$  = Partial safety factor for corrosion depth
- $Q$  = Length correction factor
- $f_u$  = Tensile strength to be used in design
- $\varepsilon_d$  = Factor for defining a fractile value for corrosion depth.

### 3.3 ANSYS Software

ANSYS Software is a finite element analysis code widely used in the computer-aided engineering (CAE) field. This software allows users to construct computer

models of structures, machine components or systems, apply operating loads and other design criteria. It permits an evaluation of a design without having to build and destroy multiple prototypes in testing. This method can reduce cost of experimental tests and minimize time taken to do analysis.

### **3.3.1 Familiarization of ANSYS**

Basic understanding of ANSYS is needed for user to know ANSYS applications and how the software works. Familiarization of ANSYS is done to introduce the user the basic and applications of the software. This process was started with preprocessor where steps of modeling, meshing, and applying constraints and loads were studied. Then, goes to solution process where analysis was done and ended with general post processing process where the results of simulation were plotted. Tutorial from ANSYS website and other tutorials in the internet [7] are referred to help in finishing this study.

### **3.3.2 Modeling**

After familiarization of ANSYS had been completed, the first step in FEA is modeling of the pipe. All models are created based on the corrosion profile and idealized corrosion pits area and later it will be properly meshed before proceeding into ANSYS simulation. The parameters used to distinguish every model are geometry of the corroded region, defect depth and analysis type.

**Nonlinear analysis:** In this study, nonlinear analysis is considered after linear analysis is completed. During failure simulation, the pipeline material is subject to large structural deformation due to loading beyond the material's yielding point. If a structure experiences large deformations, its changing geometric configuration can cause the structure to respond nonlinearly [8]. Consequently, the non-linear stress-strain relationship and the changes in geometry due to large displacement require a non-linear analysis [9].

### 3.3.2.1 Model 1: Single corrosion pit area (linear)

The first model, Model 1 (see **Figure 3.4**), was modeled by considering single defect area on the pipe. By using the advantage of symmetric boundary conditions, the dimension of the model was reduced into quarter of the pipe's dimension. The maximum corrosion depth of 4.5 mm is used as the dimension and the defect's shape area is idealized as rectangle shape, **Figure 3.5**. The model is set to linear analysis. **Table 3.2** highlights Model 1 dimensions and material properties.

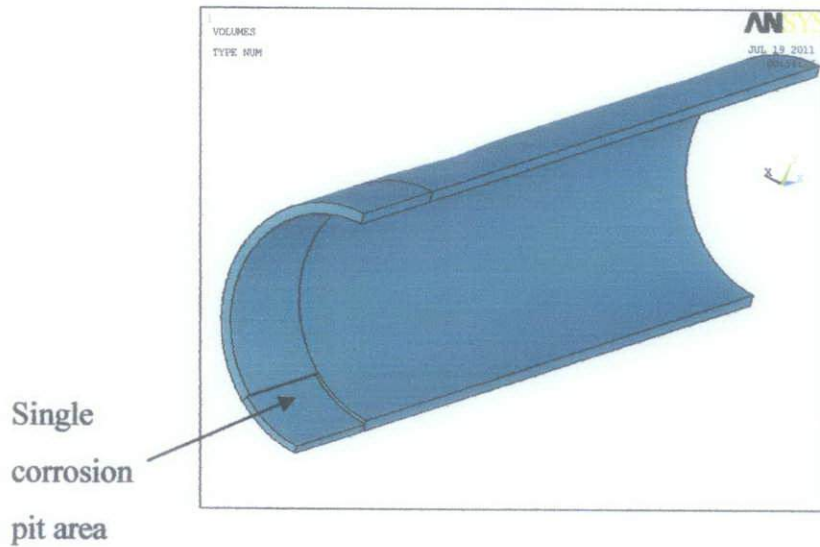


**Figure 3.4:** Model 1

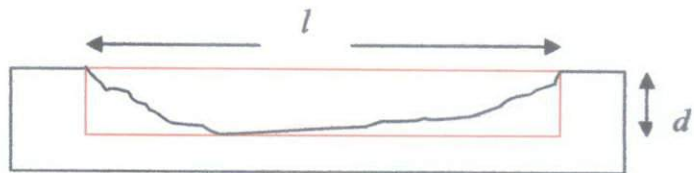


**Figure 3.5:** Idealized geometry of Model 1

**Table 3.2: Model 1 dimensions and material properties**

Actual pipe length, $L_a$ (mm)	Model's length, $L$ (mm)	Defect depth, $d$ (mm)	Corrosion pits area's length, $l$ (mm)	Young's Modulus, $E$ (GPa)	Poisson's ratio
2000	1000	4.5	150	203	0.3

### 3.3.2.2 Model 2: One major and one minor corrosion pits area (linear)

Model 2 was built by considering the 2 corrosion areas (see **Figure 3.3**), one major and one minor corrosion pit area. The maximum corrosion depth for both defects is 4.5 mm but different in defect length, as illustrated in **Figure 3.6**. **Figure 3.7** shows the idealized geometry for Model 2. The model was built into half of the pipe's dimension. **Table 3.3** shows the model's dimensions and material properties.

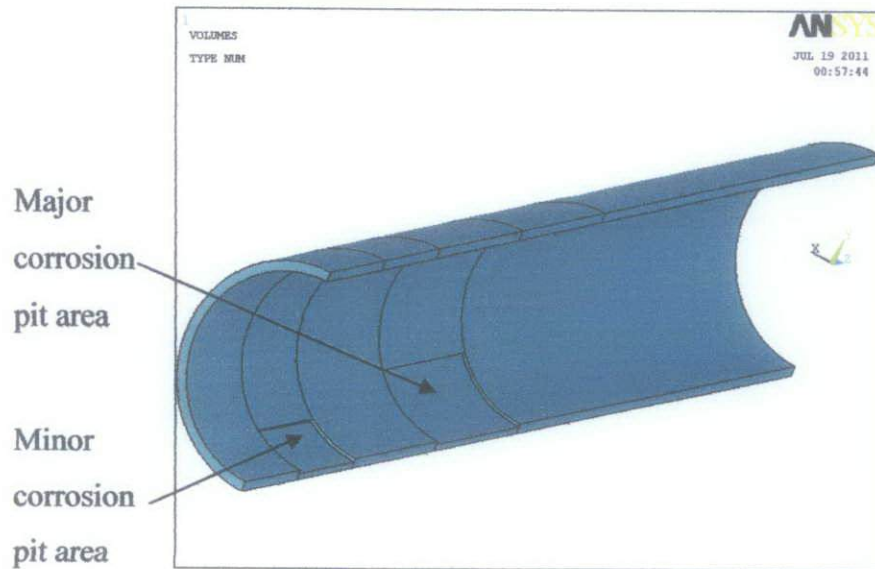


**Figure 3.6: Model 2**

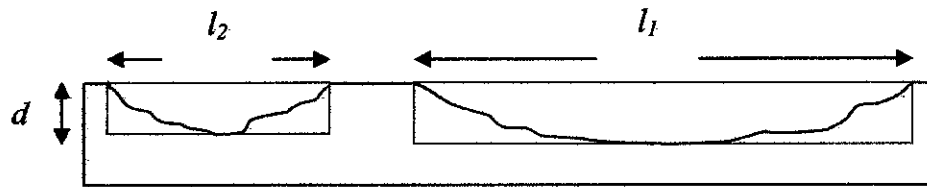


**Figure 3.7: Idealized geometry of Model 2**

**Table 3.3: Model 2 dimensions and material properties**

<b>Model's length, <math>L</math> (mm)</b>	<b>Defect depth, <math>d</math> (mm)</b>	<b>Major corrosion area's length, <math>l_1</math> (mm)</b>	<b>Minor corrosion area's length, <math>l_2</math> (mm)</b>	<b>Young's Modulus, <math>E</math> (GPa)</b>	<b>Poisson's ratio</b>
2000	4.5	300	150	203	0.3

### 3.3.2.2 Model 3: Single corrosion pit area (non-linear)

Model 3 was built with the same dimension and shape of Model 1 but the analysis is set to non-linear. In non-linear, the model was built with a set of stress-strain curve graph (see **Appendix III**) which caused the material nonlinearities when subjected to loads beyond its yielding points. This occurrence is due to large displacement experienced by the model during loading.

### 3.3.2.4 Model 4: Single corrosion pit area (non-linear)

Similar to Model 3, Model 4 was built with the same dimension, same analysis but differ in the defect depth. For this model, the defect depth used was 4mm, which was calculated as the average defect depth in the corroded region.

### 3.3.2.5 Model 5: One major and one minor corrosion pits area (non-linear)

Model 5 was built with the same dimension and shape as of Model 2 but the analysis was set to non-linear. Just like Model 3 and 4, the model was built with a set of stress-strain curve graph which resembled the material nonlinearities when subjected to loads beyond its yielding points. This occurrence is due to large displacement experienced by the model during loading.

### 3.3.2.6 Model 6: One major and one minor corrosion pits area (non-linear)

For Model 6, the dimension, geometry and analysis is the same as Model 5 but the defect depth was varied. The defect depth used was 4 mm, which was calculated as the average depth of corroded region in the pipe.

### 3.3.2.7 Model 7: Single corrosion pit area with fillet edge (non-linear)

Model 7 was built by considering the fillet around the edge of corroded region. The reason was to decrease the stress concentration of edge when subjected to internal loading. Maximum defect depth, 4.5 mm was considered in the model and the model was set to non-linear analysis.

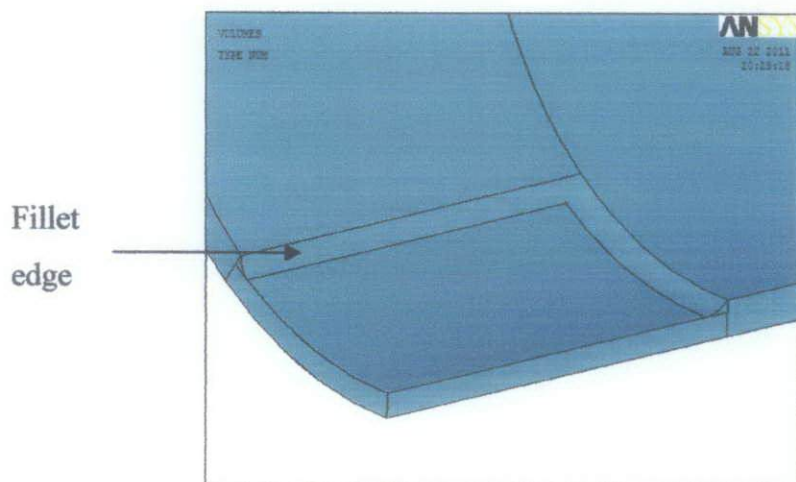
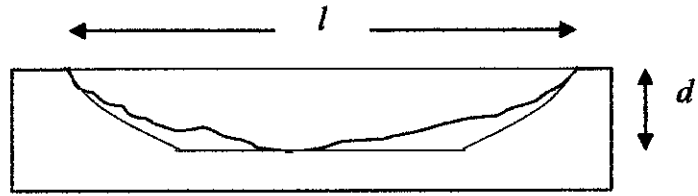


Figure 3.8: Model 7





**Figure 3.9:** Idealized geometry of Model 7

**Table 3.4:** Model 7 dimensions

<b>Actual pipe length, <math>L_a</math> (mm)</b>	<b>Model's length, <math>L</math> (mm)</b>	<b>Defect depth, <math>d</math> (mm)</b>	<b>Corrosion pits area's length, <math>l</math> (mm)</b>	<b>Fillet radius (mm)</b>
2000	1000	4.5	150	10

### **3.3.2.8 Model 8: Single corrosion pit area with fillet edge (non-linear)**

Similar to Model 7, Model 8 was built with the same geometry and analysis. The varied parameter was the depth of corroded region, where the average depth 4 mm was used as the dimension of the pipe.

### **3.3.2.9 Model 9: Single corrosion pit area, quarter of oval shape (non-linear)**

Model 9 in **Figure 3.10** is different in geometry shape compared to other models. The model was built by taking oval shape as an idealized geometry as in **Figure 3.11** and defect depth was 4.5 mm. The model was in quarter of the pipe's dimension after applying symmetric boundary conditions function.

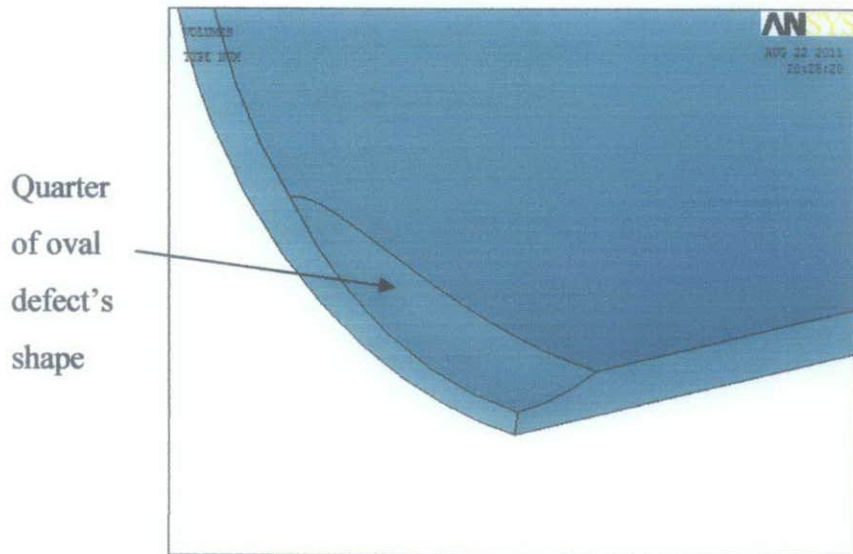


**Figure 3.10: Model 9**

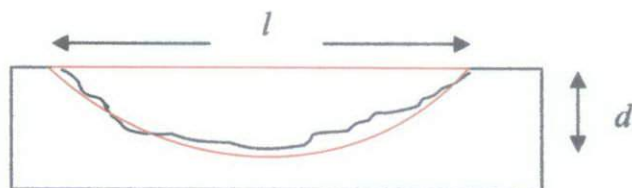


**Figure 3.11: Idealized geometry of Model 9**

### 3.3.3 Meshing

The starting point of the finite element method is subdivision. The model has to be subdivided into a finite number of smaller pieces which are called elements. These elements are defined by points at their edges called nodes. For this model the element type used was SOLID45 which is defined by 8 nodes with 3 degree of freedom (DOF) at each node. Nodes and elements together formed mesh, which approximates the shape of the real body. A fine mesh gives results that are closer to the exact solution, but the analysis is more time

consuming. As for this study, all models were properly meshed by considering the divisions of elements, aspect ratio and size of the elements. The mesh illustration for Model 1, 3 and 4 can be viewed in **Appendix IV**, Model 2, 5 and 6 in **Appendix V**, Model 7 and 8 in **Appendix VI** and model 9 in **Appendix VII**. **Table 3.7** shows the meshing properties for every model.

**Table 3.5:** Meshing properties

<b>Model</b>	<b>No. of elements</b>	<b>No. of nodes</b>	<b>DOF at each node</b>
1	3520	5004	3
2	10244	13510	3
3	3520	5004	3
4	3520	5004	3
5	10244	13510	3
6	10244	13510	3
7	4631	6612	3
8	4631	6612	3
9	13670	29240	3

### **3.3.4 Symmetric boundary condition and Loads Application**

Symmetric boundary conditions were imposed to all models. By this condition, the models can be built into half or quarter of the pipe's dimension in order to keep the calculation time as low as possible. The symmetric boundary condition reduces the complexity of model and mesh and decreases simulation time. **Figure 3.12** shows the application of symmetric boundary condition to the model.

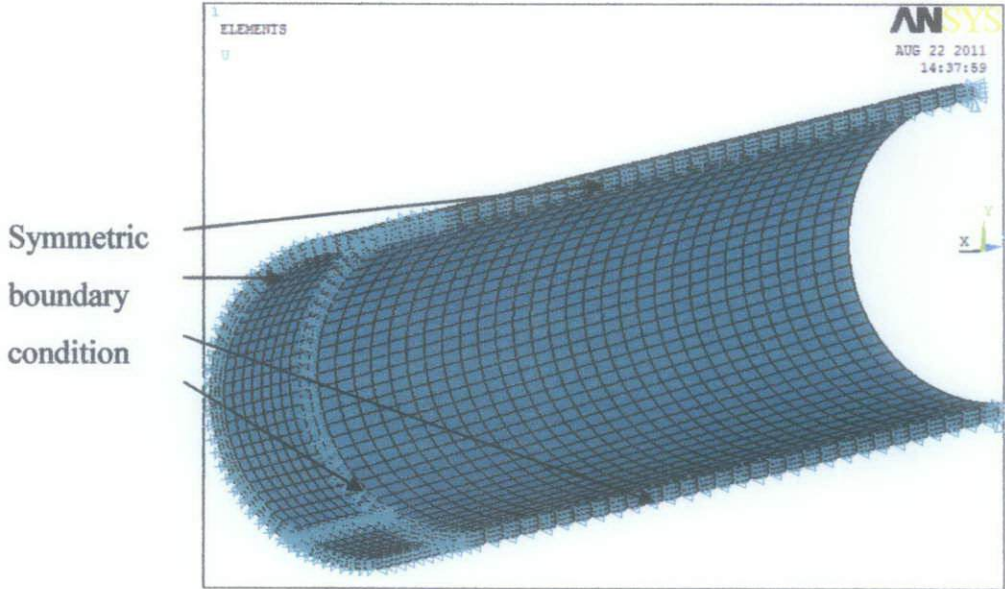


**Figure 3.12:** Symmetric boundary conditions application

Considering the operating condition of cylindrical pipe, two types of loads are implemented:

**i. Internal Pressure**

Internal pressure,  $P$  in **Figure 3.13** (red arrow) was applied to the internal surface of the model as varying parameters in the ANSYS simulation. The estimation of burst pressure,  $P_b$  can be calculated using ASME B31G (Eq.1 to Eq.3) and DNV-RP-F101 (Eq.4 to Eq.6) codes. Then, in the ANSYS simulation, the internal pressure,  $P$  is increased gradually until the Von Misses stress,  $\sigma_{VonMisses}$  of the entire nodes ligament is equal to Specified Minimum Tensile Strength, SMTS,  $\sigma_{outs}$  of the pipe. Then, the pipe is considered to burst. After that, the value of  $P$  can be considered as  $P_b$ .

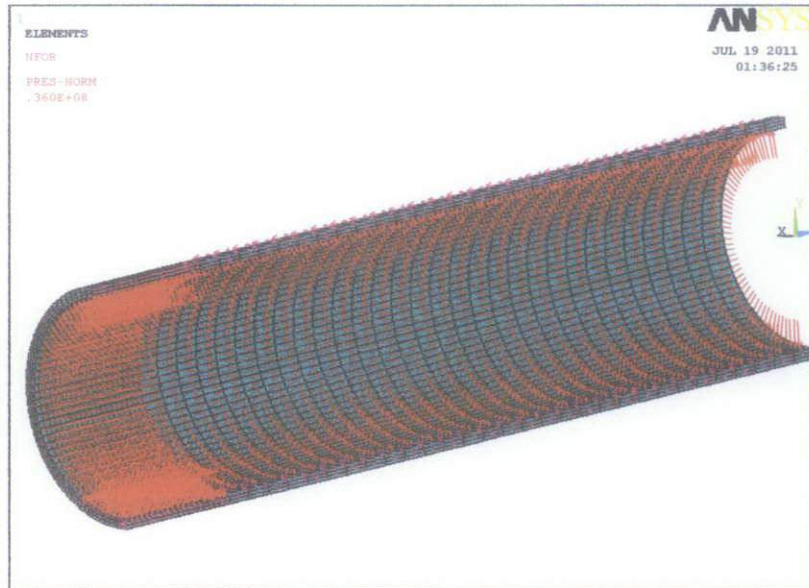


**Figure 3.13: Internal pressure loading**

## ii. Axial Tension

The axial load in **Figure 3.14** is the stress administered along the surface in the axial direction. In the model, it is subjected out of the edge of the pipe to simulate the end-caps of the burst test. The axial load can be calculated using the formula:

$$\sigma_{axial} = \frac{P * r}{2t}$$

(Eq.7)

where,

$P$  = pressure

$r$  = radius of pipe

$t$  = thickness of pipe



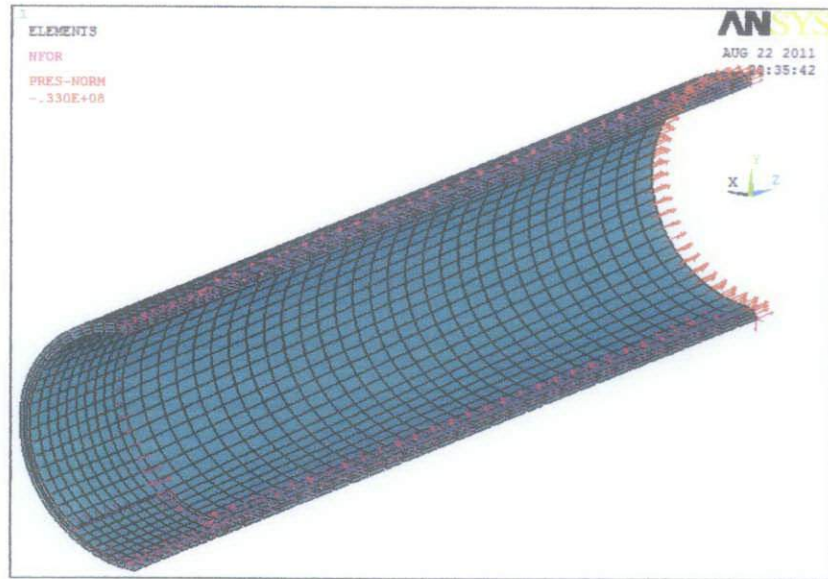


**Figure 3.14:** Axial load (red arrow)

### **3.4 Project schedule**

This project are scheduled 28 weeks effectively and divided into two phases. The Gantt charts for this project can be referred in **Appendix I and Appendix II**.

# CHAPTER 4

## RESULTS AND DISCUSSIONS

After modeling, meshing and applying all the loads to the models, the burst pressure values for every model are determined in post-processing. The models are simulated with increasing internal pressure loading,  $P$  until the Von Mises Stress,  $\sigma_{VonMises}$  of the entire nodes ligament values is equal to the Specified Minimum Tensile Strength,  $\sigma_{SMTS}$  of the pipe, 455MPa. To simulate the end-caps of the burst test,  $\sigma_{axial}$  is applied at the end of circumferential area of the models using (Eq.7).

### 4.1 ANSYS post processing results

#### 4.1.1 Model 1: Single corrosion pits area, $d= 4.5\text{mm}$ (linear)

The final result is illustrated in **Figure 4.1** and the iteration is tabulated in **Table 4.1**

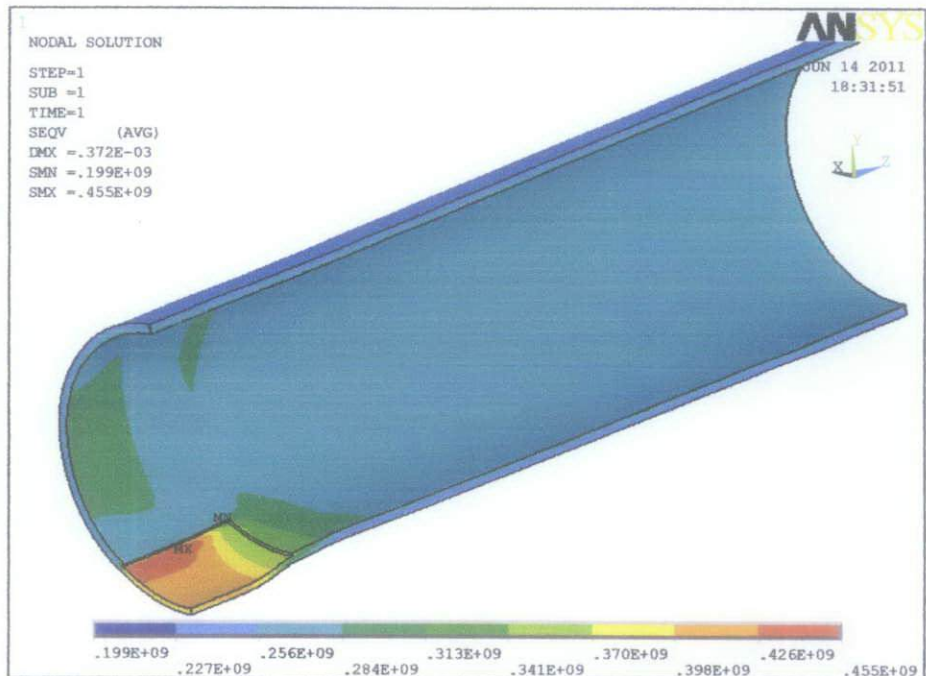


**Figure 4.1:** Von Mises plot for Model 1

**Table 4.1:** Simulation results for Model 1

<b>Trial</b>	<b>Internal Pressure loading (MPa)</b>	<b><math>\sigma_{axial}</math> (MPa)</b>	<b><math>\sigma_{VonMises}</math> (MPa)</b>
1	15	85.62	324
2	20	114.17	419
3	25	142.70	431
4	27.15	154.98	455

**4.1.2. Model 2: One major,  $d=4.5\text{mm}$  and one minor corrosion pits area,  $d=4.5\text{mm}$  (linear)**

The final result is illustrated in **Figure 4.2** and the iterations are tabulated in **Table 4.2**.

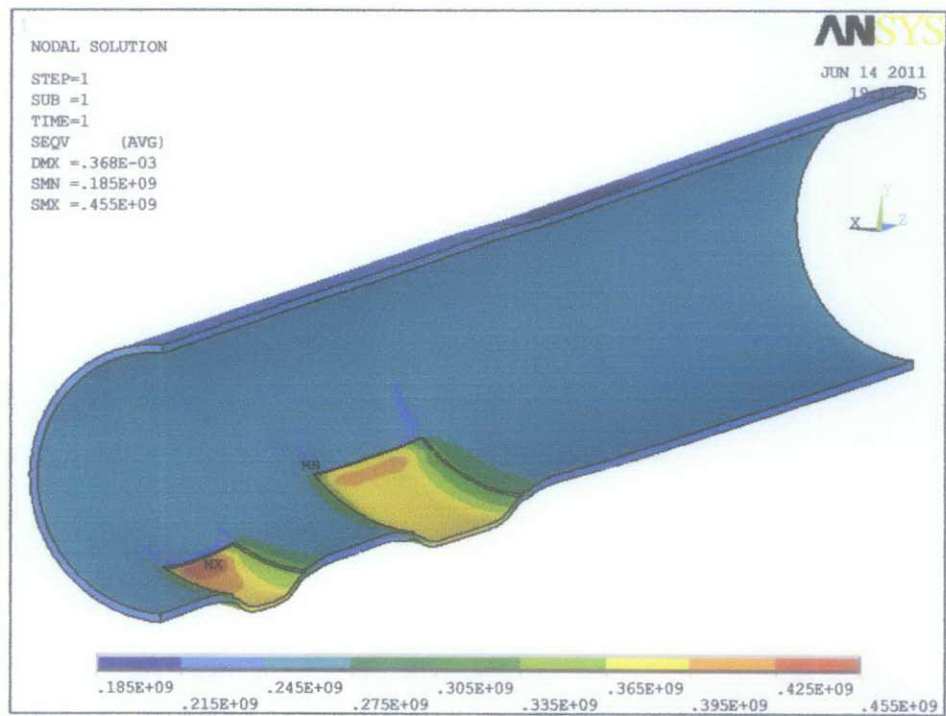


**Figure 4.2:** Von Misses plot for Model 2



**Table 4.2:** Simulation results for Model 2

<b>Trial</b>	<b>Internal Pressure loading (MPa)</b>	<b><math>\sigma_{axial}</math> (MPa)</b>	<b><math>\sigma_{VonMises}</math> (MPa)</b>
1	15	85.62	274
2	20	114.17	366
3	24	137.00	439
4	24.92	142.25	455

**4.1.3. Model 3: Single corrosion pits area,  $d=4.5\text{mm}$  (non-linear)**

The final result is illustrated in **Figure 4.3** and the iterations are tabulated in **Table 4.3**.

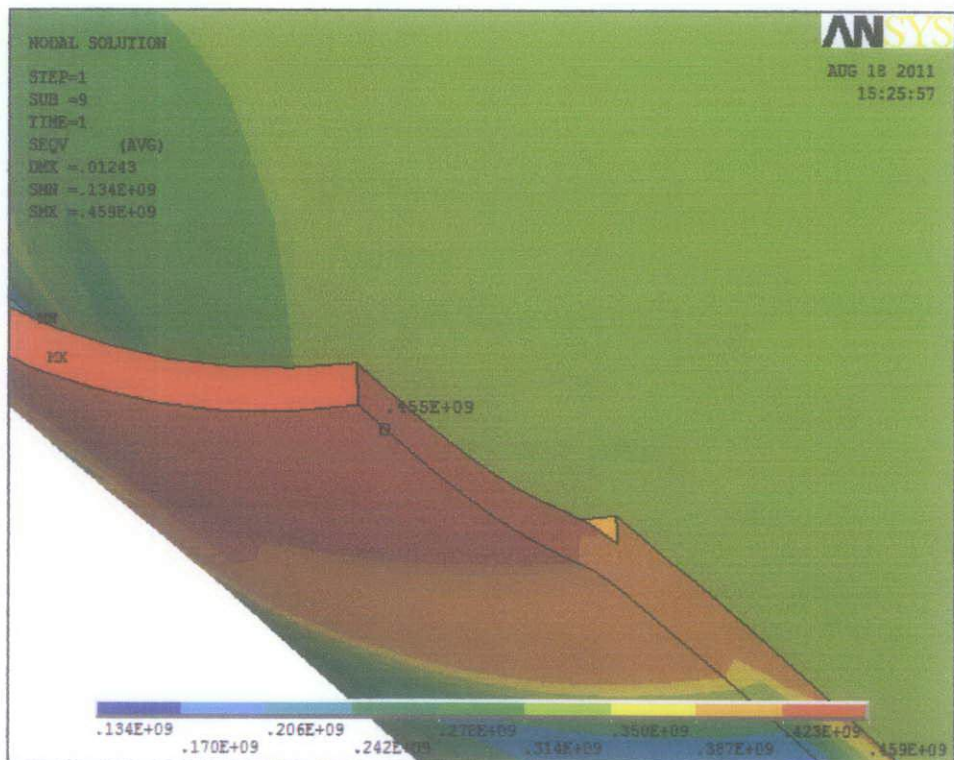


**Figure 4.3:** Von Mises plot for Model 3

**Table 4.3:** Simulation results for Model 3

Trial	Internal Pressure loading (MPa)	$\sigma_{axial}$ (MPa)	$\sigma_{VonMises}$ (MPa)
1	30	171.25	444
2	31	176.96	450
3	32	182.67	453
4	32.88	187.69	455

**4.1.4. Model 4: Single corrosion pits area,  $d=4\text{mm}$  (non-linear)**

The final result is illustrated in **Figure 4.4** and the iterations are tabulated in **Table 4.4**.

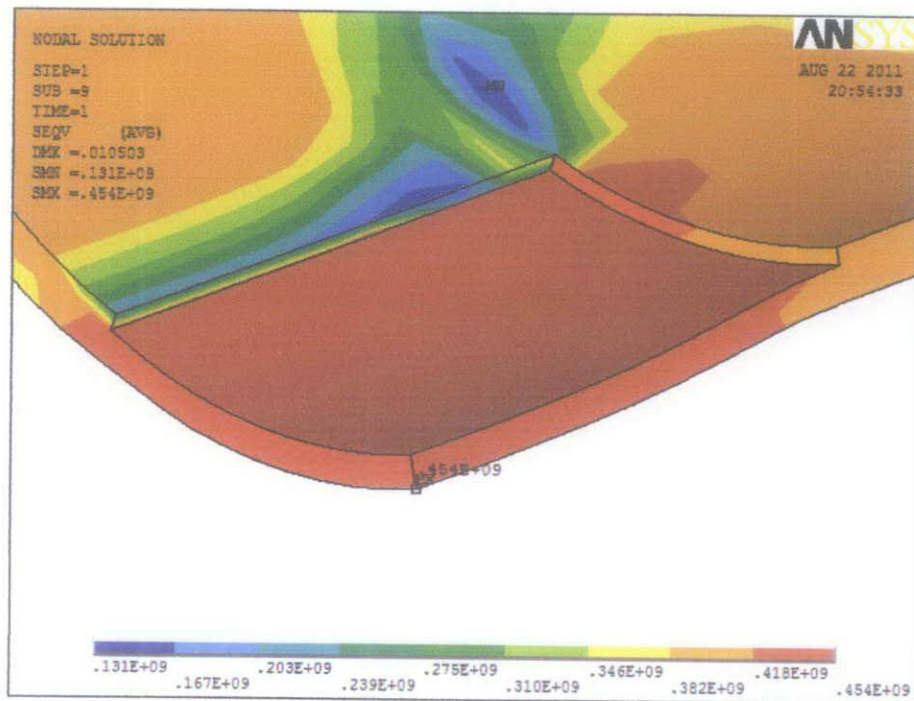


**Figure 4.4:** Von Mises plot for Model 4

**Table 4.4:** Simulation results for Model 4

<b>Trial</b>	<b>Internal Pressure loading (MPa)</b>	<b><math>\sigma_{axial}</math> (MPa)</b>	<b><math>\sigma_{VonMises}</math> (MPa)</b>
1	27.15	154.98	413
2	30	171.25	431
3	33	188.37	451
4	34.1	194.65	455

**4.1.5. Model 5: One major,  $d=4.5\text{mm}$  and one minor corrosion pits area,  $d=4.5\text{mm}$  (non-linear)**

The final result is illustrated in **Figure 4.5** and the iterations are tabulated in **Table 4.5**.

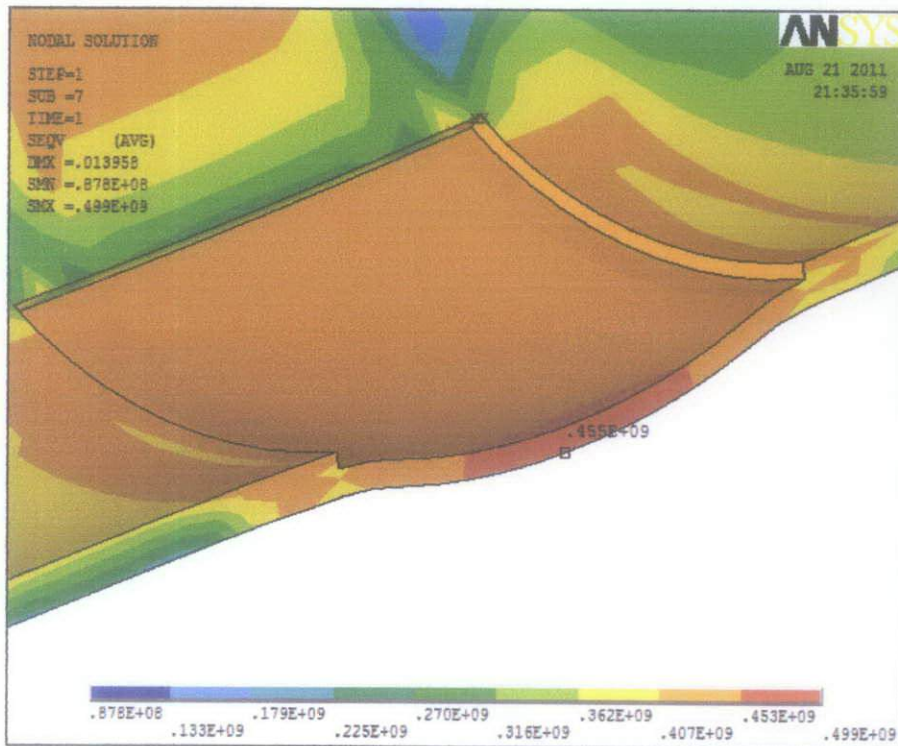


**Figure 4.5:** Von Misses plot for Model 5



**Table 4.5:** Simulation results for Model 5

<b>Trial</b>	<b>Internal Pressure loading (MPa)</b>	<b><math>\sigma_{axial}</math> (MPa)</b>	<b><math>\sigma_{VonMises}</math> (MPa)</b>
1	30	171.25	449
2	31	176.96	452
3	31.29	178.61	454
4	31.3	178.67	455

**4.1.6. Model 6: One major,  $d=4\text{mm}$  and one minor corrosion pits area,  $d=4\text{mm}$  (non-linear)**

The final result is illustrated in **Figure 4.6** and the iterations are tabulated in **Table 4.6**.

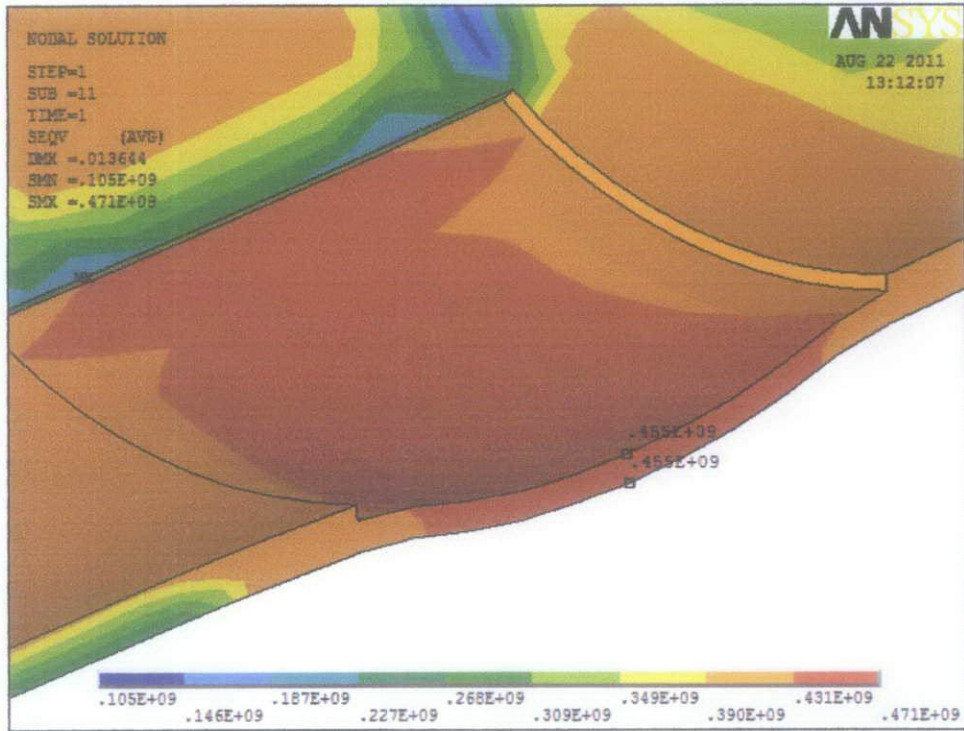


**Figure 4.6:** Von Mises plot for Model 6

**Table 4.6:** Simulation results for Model 6

<b>Trial</b>	<b>Internal Pressure loading (MPa)</b>	<b><math>\sigma_{axial}</math> (MPa)</b>	<b><math>\sigma_{VonMises}</math> (MPa)</b>
1	32	182.67	446
2	32.6	186.09	450
3	33	188.37	453
4	33.18	189.40	455

**4.1.7. Model 7: Single corrosion pit area,  $d=4.5\text{mm}$  with fillet edge, fillet radius = 10mm (non-linear)**

The final result is illustrated in **Figure 4.7** and the iterations are tabulated in **Table 4.7**.

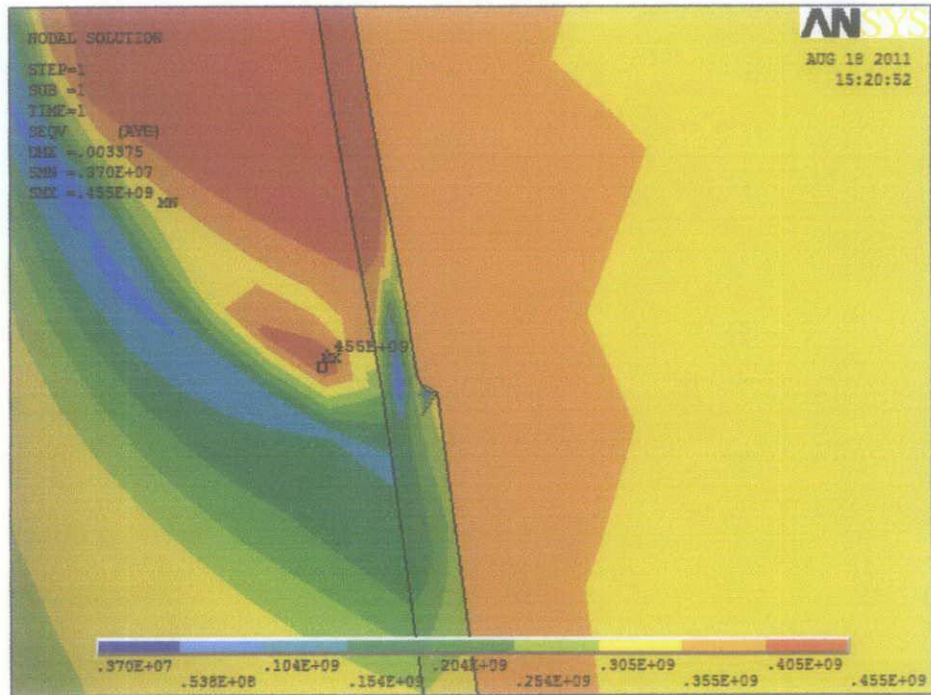


**Figure 4.7:** Von Mises plot for Model 7

**Table 4.7:** Simulation results for Model 7

<b>Trial</b>	<b>Internal Pressure loading (MPa)</b>	<b><math>\sigma_{axial}</math> (MPa)</b>	<b><math>\sigma_{VonMises}</math> (MPa)</b>
1	32	182.67	445
2	32.5	185.52	449
3	33	188.37	451
4	34.18	194.94	455

**4.1.8. Model 8: Single corrosion pit area,  $d=4\text{mm}$  with fillet edge, fillet radius = 10mm (non-linear)**

The final result is illustrated in **Figure 4.8** and the iterations are tabulated in **Table 4.8**.

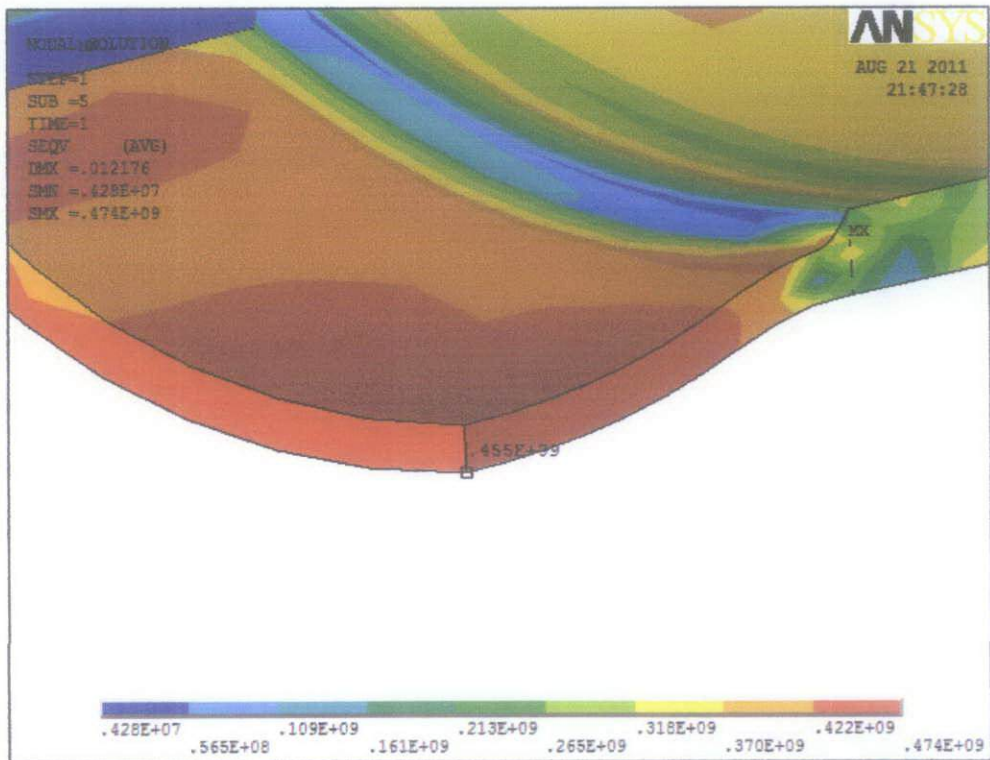


**Figure 4.8:** Von Mises plot for Model 8



**Table 4.8:** Simulation results for Model 8

Trial	Internal Pressure loading (MPa)	$\sigma_{axial}$ (MPa)	$\sigma_{VonMises}$ (MPa)
1	30	171.25	439
2	32	182.67	442
3	33.9	193.51	447
4	35.8	204.36	455

**4.1.9. Model 9: Single corrosion pit area, d=4.5mm quarter of oval shape**

**(non-linear)**

The final result is illustrated in **Figure 4.9** and the iterations are tabulated in **Table 4.9**.

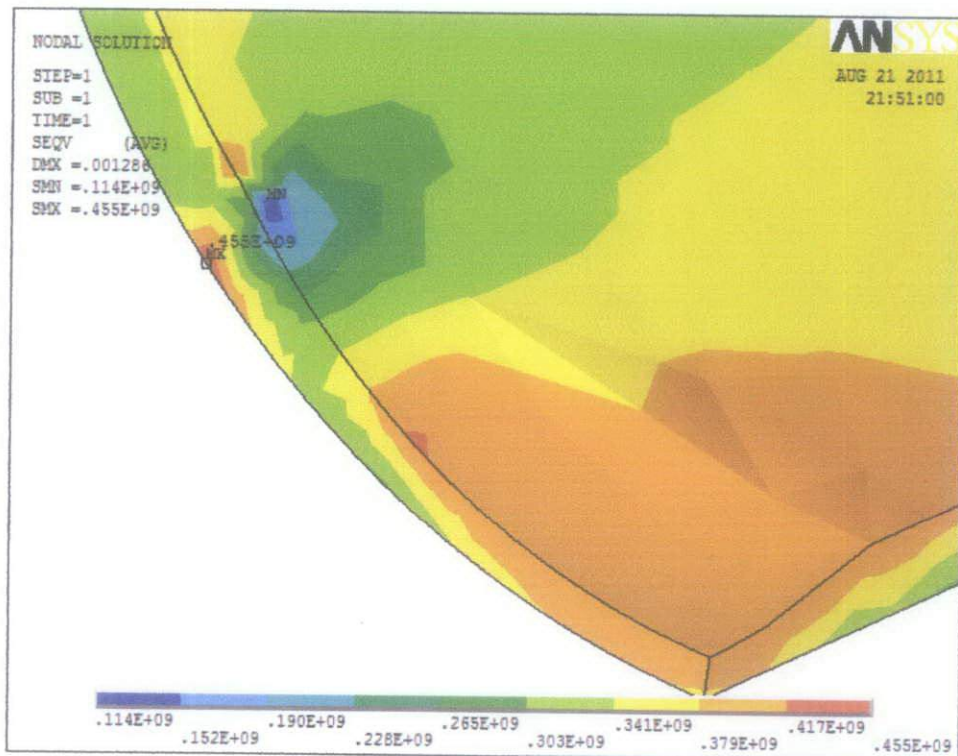


**Figure 4.9:** Von Misses plot for Model 9

**Table 4.9: Simulation results for Model 9**

<b>Trial</b>	<b>Internal Pressure loading (MPa)</b>	<b><math>\sigma_{axial}</math> (MPa)</b>	<b><math>\sigma_{VonMises}</math> (MPa)</b>
1	28	159.83	436
2	32	182.67	447
3	33	188.37	453
4	33.1	188.95	455

### 4.3 Discussions

The results for each model are tabulated in **Table 4.10** and compared to the ASME B31G, DNV-RP-F101, and the Actual Burst Test in **Figure 4.10**. From the Actual Burst Test, Maximum Allowable Burst Pressure,  $P_b$  is known to be 38.50 MPa.

From **Table 4.10**, we can see that the FEA results for Model 1 and Model 2 are much lower than the other models. Linear analysis made the models undergo linear deformations when subjected to internal pressure. Pipe material undergoes uniform deformation as well as its stress distributions. The simulation is stopped once  $\sigma_{VonMises}$  of the first node of ligament reached SMTS,  $\sigma_{SMTS}$  of the pipe.

The FEA results for models in non-linear analysis are appeared to be higher. Pipeline material is subject to large structural deformation due to loading beyond the material's yielding point. If a structure experiences large deformations, its changing geometric configuration can cause the structure to respond nonlinearly. Stress development in the pipe will increase nonlinearly too. The simulation is stopped when pipe is considered to burst after the  $\sigma_{VonMises}$  of the last nodes ligament reach SMTS,  $\sigma_{SMTS}$  of the pipe. The models involved in non-linear analysis are Model 3, 4, 5, 6, 7, 8 and 9.



For the models with maximum depth of corroded region, the  $P_b$  of the models appeared to be lower than the models with average depth of corroded region. The pressure strength of the defects is a function of its depth, therefore the deeper the defect depth,  $d$ , the lower the failure pressure. Models with maximum defect depth are Model 3, 5 and 7 while for models with average defect depth are Model 4, 6 and 8.

Geometry of the defect also plays roles in determining the  $P_b$  of the pipe. Model 3, 4, 5 and 6 which are idealized with rectangle shape plus Model 9 which is idealized with quarter oval of defect area gave lower  $P_b$  value than Model 7 and 8 which are idealized with fillet edge shape. With fillet edge, stress is less concentrated at the corner of defect area as it is concentrated at lowest thickness area of the pipe. Adding the fillet edge proved to give higher  $P_b$  result.

After comparisons is made using **Figure 4.10**, the FEA is proved to be a reliable method to estimate  $P_b$  of the corroded pipe and also the codes used, ASME B31G, and DNV-RP-F101 are also dependable codes to estimate the  $P_b$ .

**Table 4.10:** Comparisons of burst pressure,  $P_b$

<b>Burst Pressure, <math>P_b</math> results (MPa)</b>	<b>Actual burst test</b>	<b>ASME B31G</b>	<b>DNV-RP-F101</b>	<b>FEA</b>	<b>Error Comparisons FEA to Actual burst test (%)</b>
<b>Model 1</b>	38.5	22.99	32.9	27.15	29.4
<b>Model 2</b>	38.5	26.21	31.54	24.92	35.27
<b>Model 3</b>	38.5	21.55	31.14	32.88	14.6
<b>Model 4</b>	38.5	22.99	32.9	34.1	11.43
<b>Model 5</b>	38.5	24.05	29.45	31.3	18.7
<b>Model 6</b>	38.5	26.21	31.54	33.18	13.8
<b>Model 7</b>	38.5	23.76	33.46	34.18	11.22
<b>Model 8</b>	38.5	24.12	33.87	35.8	7.01
<b>Model 9</b>	38.5	30.56	35.28	33.1	14.02

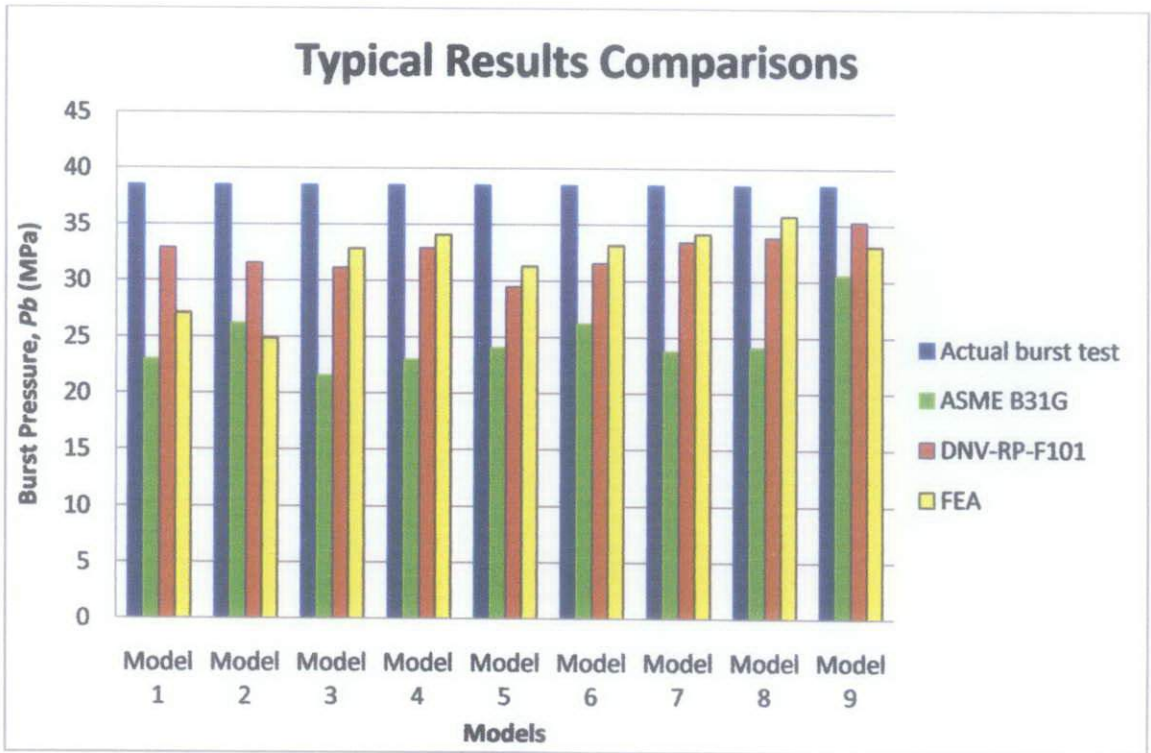


**Figure 4.10:** Comparisons of FEA to Actual burst test, ASME B31G and DNV-RP-F101

## CHAPTER 5

### CONCLUSION AND RECOMMENDATIONS

#### 5.1 Conclusion

The objectives of this study are achieved whereby the  $P_b$  value of each models are determined. Next, the best model which can represent the FEA estimation is Model 8 with  $P_b$  is 35.8MPa and lowest percentage of error, 7.01 % (see **Table 4.10**). FEA proved to be an excellent method for estimation of burst pressure of corroded pipeline which can give the result close to the actual burst test in the lab. By doing the simulation and analysis with ANSYS software, it can save cost, time, reduce the complexity of experimental procedure and reduce risk of lab work. Simulation in ANSYS is faster, reliable and user friendly. Users have flexible time of work and destructive testing can be avoided.

#### 5.2 Recommendations

Although the result is still far from the Actual Burst Test results with lowest percentage error of 7.01%, this study can be improvised from time to time. For the time being, changes and addition of defect geometry, interacting defect, and defects subjected to internal and external pressure loading can be recommended for continuation of this study. Deep study of ANSYS software is needed to widen the FEA applications and to achieve better results.

## REFERENCES

- [1] A. deS. Brasunas 1984, *Corrosion Basics: An Introduction*, Houston, Texas USA, National Association of Corrosion Engineers (NACE).
- [2] T.A. Netto, U.S. Ferraz and S.F. Estefen, "*The Effect of Corrosion Defects on The Burst Pressure of Pipelines*," Department of Ocean Engineering, Rio De Janeiro, Brazil, *Journal of Constructional Steel Research*, Issue 61, Volume 8, August 2008.
- [3] Tomasz Szary, "*The Finite Element Method Analysis for Assessing the Remaining Strength of Corroded Oil Field Casing and Tubing*," Thesis, Ph.D. Faculty of Earth Sciences, Geotechnical and Mining, Freiberg University, Germany, 10.9.2006.
- [4] M. Kamayaa, T. Suzuki, T. Meshii, "*Failure Pressure of Straight Pipe with Wall Thinning Under Internal Pressure*," Institute of Nuclear Safety System, Fukui Japan, *International Journal of Pressure Vessels and Piping*, Issue 85, 2008.
- [5] ASME, 1991, *Manual for Determining the Remaining Strength of Corroded Pipelines: A Supplement of ASME B31 Code for Pressure Piping*, American Society of Mechanical Engineers, USA.
- [6] DNV, 1997, *Reliability of Corroded Pipes Finite Element Analysis*, Report no. 96-3392, Revision no.1, Hovik, Norway.
- [7] Roosei Studio, 2004  
[http://mechanika2.fs.cvut.cz/old/pme/examples/ansys55/html/guide\\_55/g-str/GSTRToC.htm](http://mechanika2.fs.cvut.cz/old/pme/examples/ansys55/html/guide_55/g-str/GSTRToC.htm)

- [8] Belachew. C.T, M.C Ismail, K. Saravanan, "*Burst Strength Analysis of Corroded Pipelines By Finite Element Method,*" Mechanical Engineering Department, Universiti Teknologi PETRONAS, Journal of Applied Science, Issue 10: 1845-1850, 2011.
- [9] ANSYS Release 11.0, 2009, *ANSYS Structural Analysis Guide*, ANSYS Inc. Canonsburg, PA.
- [10] J.B. Choi, B.K. Goo, J.C. Kim, Y.J. Kim, W.S. Kim, "*Development of Limit Load Solutions for Corroded Gas Pipelines,*" Int. Journal of Pressure Vessels and Piping 80: 121-128, 2003.
- [11] G.S. Ping Carina. "*Burst Test Simulation of Corroded Pipelines.*" Thesis, Mechanical Engineering Department, Universiti Teknologi PETRONAS, 2010.
- [12] Roberge, Pierre R. 2007, *Corrosion Inspection And Monitoring*, Ontario, Canada, John Wiley & Sons.





## Appendix II: FYP II Project Gantt Chart

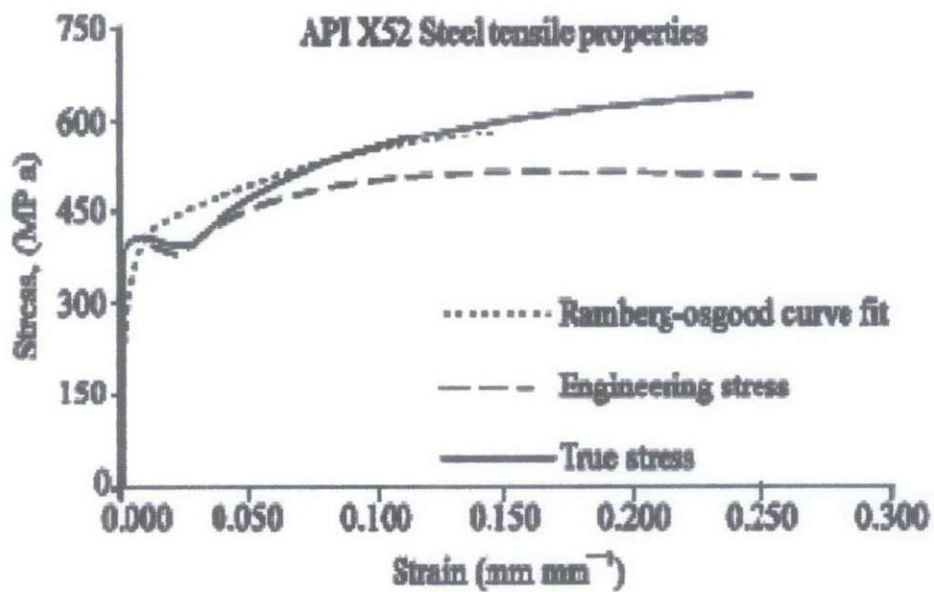
No.	Activities	Week													
		1	2	3	4	5	6	7	8	9	10	11	12	13	14
1.	Remodeling Model 1	█													
2.	Build Model 1 (linear) Single corrosion pits area, $d=4.5\text{mm}$  2.1 Meshing of Model 1. 2.2 Applying symmetric boundary conditions. 2.3 Applying internal pressure load and axial load. (repeat activities 2.1, 2.2, 2.3 for all models after building the model)		█												
3.	Build Model 2 (linear) One major, $d=4.5\text{mm}$ and one minor corrosion pits area, $d=4.5\text{mm}$			█	█										
4.	Build Model 3 (non-linear) Single corrosion pits area, $d=4.5\text{mm}$					█	█								
5.	Build Model 4 (non-linear) Single corrosion pits area, $d=4\text{mm}$							█	█						
6.	FEA Results comparison to actual burst test.								█						
7.	Build Model 5 (non-linear) One major, $d=4.5\text{mm}$ and one minor corrosion pits area, $d=4.5\text{mm}$									█	█				
8.	Build Model 6 (non-linear) One major, $d=4\text{mm}$ and one minor corrosion pits area, $d=4\text{mm}$											█	█		
9.	Build Model 7 (non-linear) Single corrosion pit area,												█	█	

Mid-Semester Break

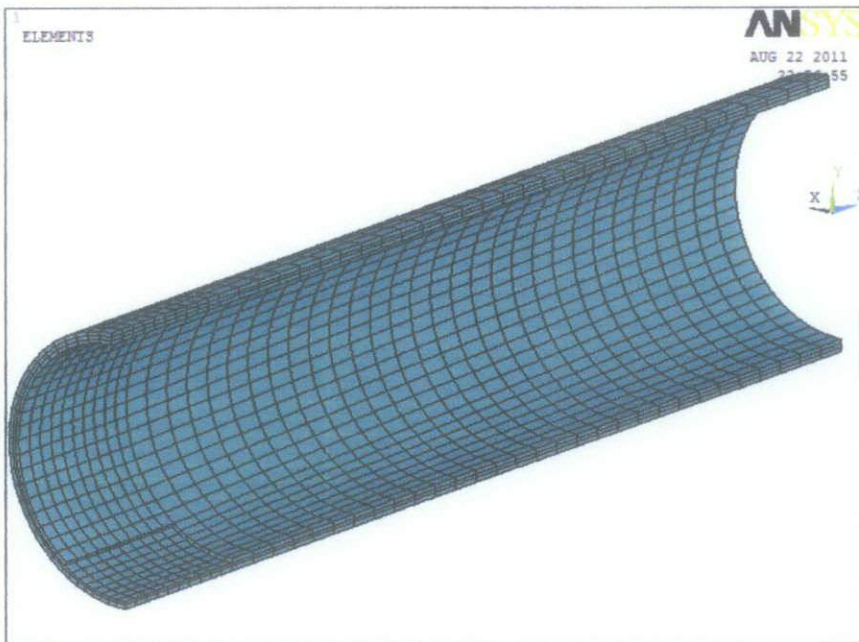




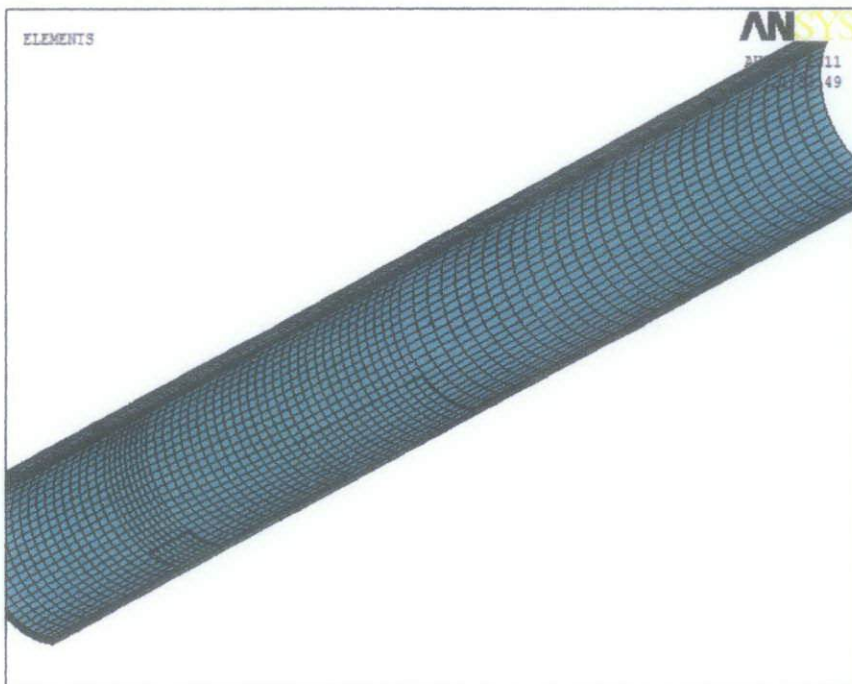
Appendix III: Tensile Properties of API X52 grade steel [6]



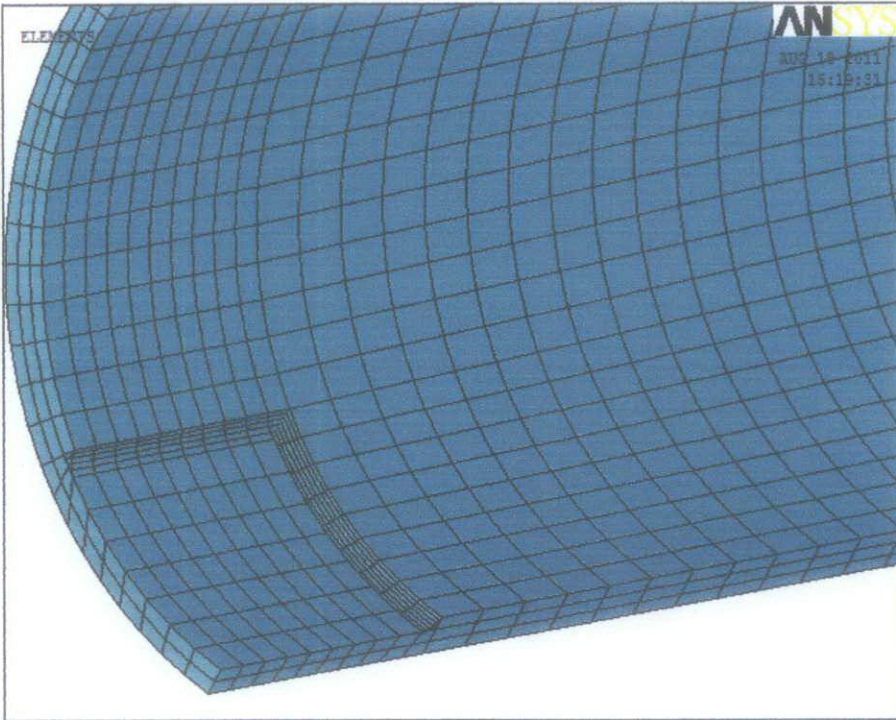
#### Appendix IV: Mesh of Model 1, 3 and 4



#### Appendix V: Mesh of Model 2, 5 and 6



## Appendix VI: Mesh of Model 7 and 8



## Appendix VII: Mesh of Model 9

